Dabaja *et al. Cell Biosci (2018) 8:47*
https://doi.org/10.1186/s13578-018-0243-1

Cell & Bioscience

RESEARCH

Open Access

Metabolic alterations induced by attenuated Zika virus in glioblastoma cells

Mohamed Ziad Dabaja[1†], Estela de Oliveira Lima[1†], Diogo Noin de Oliveira[1†], Tatiane Melina Guerreiro[1], Carlos Fernando Odir Rodrigues Melo[1], Karen Noda Morishita[1], Marcelo Lancellotti[2], Ana Lucia Tasca Gois Ruiz[3], Gisele Goulart[3], Diego Andreazzi Duarte[4] and Rodrigo Ramos Catharino[1*]

Abstract

Background: Zika virus (ZIKV) has recently become a major matter of concern since its association with microcephaly cases in newborns was determined. From then on, ZIKV has been untiringly studied, and several scientific data have shown the virus' tropism to neural cells. Previous studies have proposed that ZIKV induced glioblastoma cells death, suggesting that ZIKV and ZIKV-associated molecules might induce intracellular biochemical alterations, and thereby be alternatives for neural cancer management. In this sense, the present contribution presents a prospective approach for glioblastomas management: producing a ZIKV-based therapy that stimulates glioblastoma control. We developed an attenuated ZIKV prototype based on bacterial outer membrane vesicles (OMV). The attenuated ZIKV was applied on glioblastoma cells, where cytopathic and cytostatic effects were evaluated. Glioblastoma cells, with and without treatment, were submitted to mass spectrometry analysis.

Results: Microscopic analysis showed cytopathic effects induced by ZIKV prototype on glioblastoma cells after 24 and 48 h post-treatment. DNA fragmentation assay and TNF-alpha expression were indicative that ZVp induced cell damage and death. The metabolomics investigation elected 5 different biomarkers that might be associated with cell cytopathic effects, highlighting intracellular biochemical modifications induced by the attenuated ZIKV. The remarkable evidence of cell death in glioblastoma stimulated further studies that rendered a preliminary screening with other tumor cell lineages, though anti-proliferative activity test. Among the 11 tumors evaluated, prostate and ovarian tumors were the most affected by ZIKV prototype, and other 6 cell lines also presented cytostatic effects.

Conclusions: Results ultimately demonstrated that this prototype not only emerges as a potential alternative for glioblastoma management, but may also be an important tool against other important tumors.

Keywords: Zika virus, Outer membrane vesicle, Prototype, Mass spectrometry, Cancer research

Background

In the last 2 years, the absence of profound knowledge about ZIKV has encouraged intense research all over the world. Scientific investigations are stimulated mainly due to the serious impact over neural development of fetuses from mothers who were infected by ZIKV during pregnancy [1, 2], as well as the Guillain–Barre syndrome that may affect adult infected individuals, although to a lesser extent. Recent studies have focused on disclosing intracellular processes alterations as well as the biochemical pathways modified by viral infection. Some of them have shown that ZIKV infection increased cell-cycle deregulation and cell death rates in vitro, in human neural progenitor cells (hNPCs), in addition to apoptosis activation associated with deregulation of DNA transcription [3]. Transcriptome analyses, evaluated by McGrath et al. [4] in human fetal brain-derived neural stem cells infected with ZIKV, have revealed the down-regulation of genes associated with cell-cycle and neurogenesis, while genes involved with apoptotic cell death and innate immunity

*Correspondence: rrc@g.unicamp.br; rrcatharino@gmail.com
†Mohamed Ziad Dabaja, Estela de Oliveira Lima and Diogo Noin de Oliveira contributed equally to this work
[1] Innovare Biomarkers Laboratory, School of Pharmaceutical Sciences, University of Campinas-UNICAMP, Campinas, SP, Brazil
Full list of author information is available at the end of the article

were up-regulated. Most recently, mechanistic insights have been shown by Devhare et al. [5] who evaluated two ZIKV strains that displayed different growth rates in hNSCs. Although these two ZIKV strains presented different cellular mechanisms, both induced death, either through DNA damage, caspase-3 cleavage or increased p53 activity.

According to the examples cited above, the focus of ZIKV scientific research has been upon its effects on neural progenitor/stem cells, mainly due to the evidences of viral neural tropism. However, new insights have emerged: ultimately, Zhu et al. [6] and Lima et al. [7] have considered ZIKV cell death associated with tropism for progenitor neural cells as a useful approach for neural tumor management. Their work showed that ZIKV is capable of infecting and effectively killing glioblastoma stem cells in comparison to normal neuronal cells, differently from other neurotropic viruses such as West Nile virus, which induces cell death in both normal and tumor neural cells. Their findings suggest that genetically modified ZIKV would be a viable therapeutic strategy for glioblastomas control, as it is the most aggressive and chemoresistant neural tumor reported to date [6, 7].

While genetic engineering of ZIKV would be an interesting alternative as oncolytic strategy, since the exact mechanism of ZIKV neuropathogenesis is still not well-described, the exact modifications needed in viral structure to produce an assertive and safe oncolytic virus remains impaired. Although tumor management through virotherapy is a promising strategy, safety issues such as unexpected toxicities, virus mutability and transmissibility, and healthy cells elimination [8, 9] must be understood and considered, as well as the triggering factors for Guillain–Barre syndrome, in the case of ZIKV.

Taking into account previous literature background that provide basis for the use of ZIKV specifically in neural cancer therapy, and potential safety issues concerning an oncolytic bioengineered ZIKV, we hereby propose an attenuated Zika virus prototype (ZVp) with viral fragments encapsulated into the OMVs of *Neisseria meningitidis* as an alternative to cancer management.

Results

Cytopathic effects of ZVp in GBM cells

Intending to evaluate cytopathic effects of the ZVp on neural cancer cells, human malignant U-251 glioblastoma cells (GBM) were divided into four different groups, which received distinct treatments, including a medium-only specimen (control group—CT), empty OMV, ZIKV and ZVp. All groups were evaluated through bright field microscopy in two timepoints of infection: 24 h and 48 h. In addition, after 24 h of infection, all groups were also submitted to Wright staining microscopy analysis (Additional file 1). Thus, the first timepoint evaluated showed that treatment with ZVp induced mild cytopathic effects, represented by morphological alterations as round, swollen cells, syncytium formation, cytoplasm fragmentation and chromatin condensation (Fig. 1d and Additional file 1: Figure S1d). All of these effects were milder in OMV and ZIKV groups, but non-existing in the control group (Fig. 1a–c and Additional file 1: Figure S1a–c). After 48 h of treatment, ZVp group (Fig. 1h) presented shape-altered cells, loss of cellular integrity and notably fewer cells compared to other groups (Fig. 1e–g), which

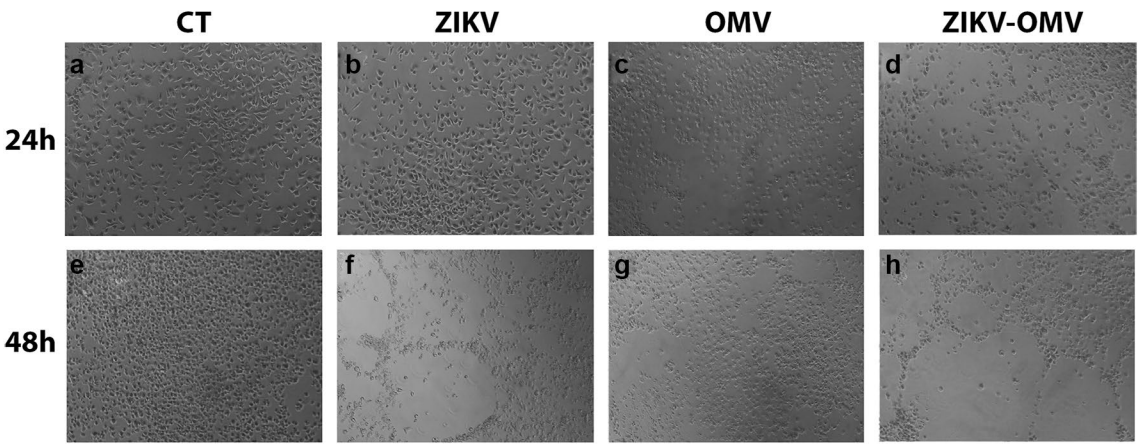

Fig. 1 Cytopathic effects of the ZVp in glioblastoma cells. Glioblastoma cells, submitted to four different treatments, were evaluated through bright field optical microscopy performed at 24 and 48 h post-infection. **a**–**d** Are microscopic images made at 24 h post infection, and **e**–**h** are their counterparts, 48 h post infection. The groups were: control (CT); empty outer membrane vesicle (OMV); wild-type Zika virus (ZIKV); attenuated Zika virus prototype (ZVp), respectively scale bars, 100 µm

highlights substantial cytopathic effects induced in the second timepoint of treatment with ZVp.

In addition to cytopathic effects, it was possible to evaluate DNA fragmentation in all four groups, 24 h after infection (Additional file 1: Figure S2), evidencing that ZVp-treated cells presented putatively increased DNA damage compared to all other groups. The same evaluation was not performed for the later timepoint of infection due to reduced mRNA extracted from treated samples, given that ZIKV and ZVp presented intense reduction of cells.

Corroborating with these observations, we have also evaluated TNF-alpha expression through qRT-PCR. This semi-quantitative analysis showed that ZVp presents higher TNF-alpha expression (Additional file 1: Figure S3). Although it was not statistically significant compared to the other groups, ZVP presents an important tendency in inducing overexpression of TNF-alpha cytokine.

Biomarkers identification through ESI-HRMS analysis

Intending to elucidate biochemical mechanisms involved with the cytopathic effects, we performed a comparative metabolomics analysis between glioblastoma CT and ZVp groups, after 24 h of treatment. Intending to achieve metabolites responsible for triggering cell cytopathic effects, metabolomics analysis has prioritized to perform the biomarkers elucidation in the first timepoint of the ZVp treatment. In this way, it is possible to know exactly how to interfere in tumors to induce cell death in a further phase. The data obtained from mass spectrometric analysis were submitted to a PLS-DA, which pointed differences between metabolite composition in CT cells versus attenuated ZIKV treated cells (Additional file 1: Figure S4). From a threshold value of 3.1 in VIP scores, biochemical markers for the ZVp-treated group were highlighted. The proposed prototype supported the election of five different biomarkers for the ZVp-treated group, illustrated in spectral Fig. 2. Among elected markers we found three chlorinated phospholipids: lysophosphatidic acid ($m/z = 473$), an oxidized phosphatidylserine ($m/z = 652$) and a simple phosphatidylserine ($m/z = 586$), a chlorinated metabolite of the folate pathway, 5-methyltetrahydropteroyltri-L-glutamate ($m/z = 675$), and a deprotonated Phosphatidylinositol-3-phosphate ($m/z = 1049$; all in Additional file 1: Table S2).

Anti-proliferative ZVp assay

To investigate any possible effects of the ZVp upon proliferation in glioblastomas and expand this investigation to different tumor lines, the anti-proliferative activity of ZVp was evaluated (Additional file 1: Figure S5), which was expressed as the sample concentration, in OMV mL^{-1}, required to produce 50% of cell growth inhibition (GI_{50} value). Other parameter calculated was the selectivity index (SI) that is an indicator of anti-proliferative effect on normal tissues although, as an on-target toxicology indicator (the expected drug effect), it was not able to predict other systemic toxic effects (Additional file 1: Table S1). According these parameters, the ZVp showed a selective cytostatic effect against prostate (PC-3, $GI_{50} = 14.7 \times 10^6$ OMV mL^{-1}, SI = 40.1) and ovarian (OVCAR-03, $GI_{50} = 149.5 \times 10^6$ OMV mL^{-1}, SI = 3.9) tumor cell lines, whilst showed potential to inhibit cell growth in 50% of tumor cell lines U251, NCI ADR/RES, 786-O and HT-29 and immortalized cell line HaCat.

Discussion

Results support the potential of using an attenuated ZIKV for the control of glioblastomas and other tumor cell lines, whilst bring into focus novel biochemical markers associated with tumor anti-proliferative effect induced by ZIKV particles associated with *N. meningitidis* outer-membrane vesicles. The first evidence pointed out was the cytopathic effect observed after treatment of U-251 glioblastoma cells with the ZVp, even 24 h or 48 h post-attenuated ZIKV inoculation (Fig. 1 and Additional file 1: Figure S1). In addition to microscopic evidences, DNA fragmentation assay indicates that ZVp induced DNA damage in glioblastoma cells (Additional file 1: Figure S2), which is coherent with the tendency of TNF-alpha overexpression (Additional file 1: Figure S3), associated with double-stranded DNA fragmentation [10, 11]. TNF-alpha is also an important cytokine that acts in tissue homeostasis and immune response regulation [12]. Considering that this cytokine is described as tumor necrosis inductor [13], also through Caspase-3 activation [14], it is possible to infer that ZVp might be activating the TNF-alpha synthetic pathway. Therefore, it is plausible that glioblastoma cells death be induced by biochemical intracellular pathways mediated/activated through TNF-alpha.

In line with the toxic effects of ZVp observed in the present research, previous studies have shown cell survival rate and cycle alterations due to ZIKV infection in glioblastoma cells, where tumor cells infected with ZIKV showed cytopathic effects [7] and apoptosis [6]. In addition to caspase-3 activation, shown by Zhu et al., some studies have also shown that apoptosis induced by ZIKV might be associated with perturbation of Toll-like receptors-3 (TLR3) network [15] and consequent inhibition of Sonic Hedgehog and RAS-ERK signaling [16]. Inhibition of these biochemical pathways could result in cell cycle arrest and blockage of cell proliferation, as well as induction of cell death [17, 18], which is coherent with cytostatic and cytopathic results observed in the present study.

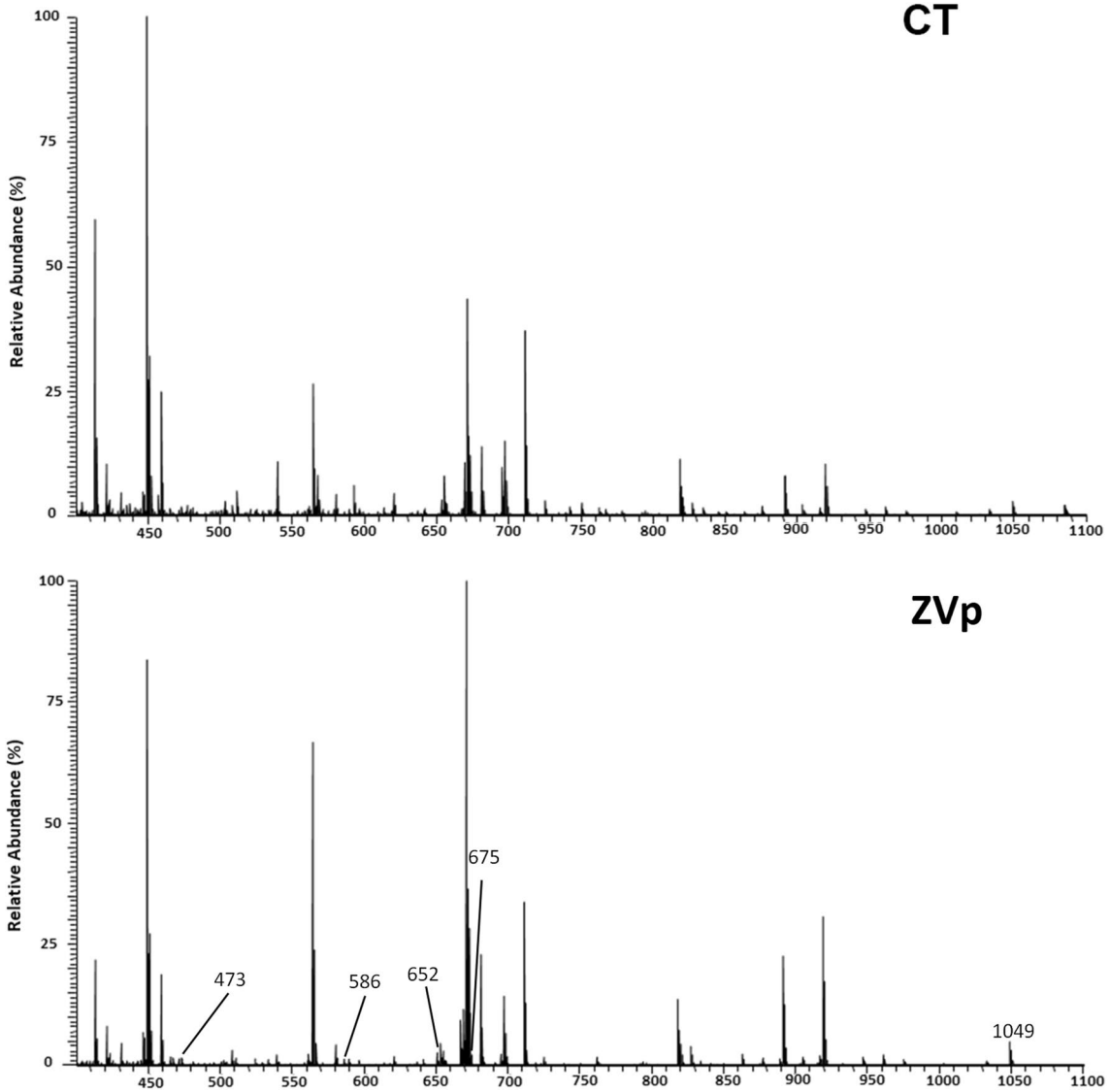

Fig. 2 Representative fingerprinting of the control (CT) and ZIKV prototype treated (ZVp) glioblastoma cells (ZIKV), 24 h post-treatment. The imaging represents a sum of all ions within mass range *m/z* 400–1100 on negative ion mode. The ion indications correspond to the identified biomarkers shown in Additional file 1: Table S2

Other results support that the ZVp may also activate other Toll-like receptors (TLRs), since bacterial outer membrane vesicles present lipopolysaccharide (LPS), known as a potent activator of Toll-like receptor 4 (TLR4) [19]. Upon LPS-TLR4 activation, several studies have demonstrated that LPS-TLR4 interaction induces reactive oxygen species (ROS) production through activation of NADPH oxidase (Nox) [20, 21]. In addition to oxidative environment is indicative of biochemical imbalance, it may also be neurotoxic and induce cell death [22, 23]. These alterations support the oxidative ambient induced by the ZVp observed in our research, where metabolomics analysis allowed the identification of an oxidized phosphatidylserine (PS) ($m/z = 652.2$); in contrast, a non-oxidized PS ($m/z = 586.2$) was also identified. It is well-known that PS exposure on the outer layer of cell membrane is indicative of apoptotic cells, working as specific markers for phagocyte recognition and removal [24, 25]. Therefore, PS identification may also be a consequence of cell death induced by ZVp.

In addition to ROS, inducible nitric oxide synthase (iNOS) is upregulated in microglia cells when under pathological conditions as viral infections, corroborating an intracellular environment of oxidative stress [22, 26, 27]. Nitric oxide (NO), a product of iNOS, has been reported as a regulator of carbon flow through the folates pathway, as NO binds to cobalamin (oxidation) and inhibits its role as a cofactor of methionine synthase (MS) [28, 29]. 5-Methyltetrahydropteroyltri-L-glutamate, an elected biomarker for the ZVp-treated group, is involved in homocysteine remethylation to methionine mediated by MS. Considering that MS activity is inhibited by oxidized cobalamin under oxidative conditions, the metabolite 5-methyltetrahydropteroyltri-L-glutamate may accumulate, thereby indicating alterations in the one-carbon transfer reactions mediated by the folate pathway. The folate-mediated synthesis of methionine is crucial for DNA methylation and production of purines and pyrimidines, as folate is responsible for providing one-carbon (methyl) blocks for nucleotide synthesis [30, 31]. Hence, it is possible to infer that our ZVp was able to negatively interfere on DNA methylation and nucleotide synthesis, favoring cell cycle arrest, chromosome instability and, ultimately, cell death [32–34].

Moreover, phosphatidylinositol trisphosphate (PIP3) was also identified in glioblastoma cells treated with the ZVp. A recent contribution by our group has also observed phosphatidylinositol phosphates among ZIKV biomarkers [35], corroborating our findings. Usually, under pathogens challenge, Akt-mTOR might be activated through TLR4 stimulation, what happens under LPS stimulation [36–38]. However, according to Liang et al. [39], ZIKV presents two non-structural proteins (NS4A and NS4B) that suppress the Akt-mTOR pathway signaling. Thus, it is possible to infer that TLR4 activates phosphatidylinositol-3-kinase (PI3K), which increases PIP3 availability, but without success in signaling cascade proceeding, taking into account that ZIKV proteins are capable of inhibiting Akt-mTOR complex, the final target of PIP3. Therefore, phosphatidylinositol trisphosphate accumulates due to the constant TLR4 activation by attenuated ZIKV prototype antigens and becomes an evident biomarker in our experiment.

Taking into account that microglia cells were the target of mass spectrometric analysis in this study, we must consider their particular characteristics. Microglia cells are the neuroprotective and immunocompetent ones among glial cells [40, 41], and can be activated by extracellular stimuli and under injury conditions, represented here by the ZVp. Once activated, microglia cells undergo for profound morphological and biochemical changes, culminating with synthesis of bioactive molecules. Lysophosphatidic acid (LPA) is a bioactive phospholipid and is abundantly present in brain cells [42, 43]. Under microglia activation, LPA concentration increases due to oxidative damage, and phospholipases activation, which catalyzes LPA production [44, 45]. Concerning the present study, LPA was one of the biomarkers identified for glioblastoma cells under treatment with the ZVp. In face of the oxidative previous explanation and the infectious environment simulated by the attenuated ZIKV, it is plausible to infer that LPA production was increased. Some studies have also shown that LPA induces cell death by modulating redox environment or through upregulation of tumor necrosis factor receptor [46, 47]. Therefore, it is possible that the primary redox imbalance induces LPA synthesis and subsequently LPA itself contributes to intensify the intracellular oxidative environment. Furthermore, TNF has also been related as a neuronal cell death inductor stimulated by ZIKV [48]. ZVp presents ZIKV inactivated by heat, thereby not excluding the presence of ZIKV antigens, even inactivated; hence, it is possible that ZIKV antigens may still sensitize cellular response and induce immune response. Thus, LPA may be involved in induction of cell cytopathic effects observed in our study.

In addition to metabolic alterations induced by the ZVp over glioblastoma cells, we have also intended to confirm its cytopathic effects over the same cell line and evaluate its potential over several other sorts of tumors. Therefore, we have performed a preliminary anti-proliferative activity test over glioblastomas and eight other different cell lines. This first test confirmed the anti-proliferative effect of the ZVp over GBMs, since it showed 50% of cytostatic effect. Interestingly, the attenuated ZIKV prototype cytostatic effect has also been observed in six other tumors and one immortalized cell lines. Noteworthy, the most affected cell lines were prostate and ovarian tumor cells, where cytostatic effect was most evident. It has been recently observed that ZIKV presents tropism for urogenital cells [49–51], and our results show that the ZVp presented a similar tropism, even after inactivation by heat. Although prostate and ovarian cells were the most affected, the attenuated ZIKV prototype still presents potential to interfere with other 6 cell lines that have also shown cytostatic effect, mainly glioblastoma, which is the most studied cell line with respect to ZIKV infection.

Conclusions

All these findings allowed us to propose a number of altered biochemical pathways in tumor cells during the ZVp treatment. The most interesting data shown by the

present study is the possibility of using an attenuated ZIKV based into ZIKV for management of glioblastomas, expanding its potential to be applied for management of different tumors. The advantages of using this method consists of the immune protection provided by it and the lower cost compared to virus genetic modification. This study is a window that opens for further researches, such as in vitro adjustment of attenuated ZIKV doses, in vivo tests of viability into animals' tumors and applications in human cancer management.

Methods

Attenuated ZIKV prototype development

Neisseria meningitidis (C2135); *Aedes albopictus* (C6/36) and glial cells (M059J) were the cell lines used in this study, all obtained from (INCQS—FIOCRUZ—National Institute for Quality Control—Oswaldo Cruz Foundation, Rio de Janeiro, RJ and Cell Bank). The ZIKV strain used in the present study corresponds to Brazilian ZIKV strain (BeH823339, GenBank KU729217), which was isolated from a patient in the State of Ceará (Brazil) in 2015. The viral strain was gently provided by Professor Doctor Edison Durigon (Biomedical Sciences Institute, University of São Paulo).

Each cell line was grown under the following conditions: M059J cells line were submitted to cultivation with RPMI1640 medium supplemented with 10% of fetal bovine serum (FBS) and 1% of antibiotics (tetracycline 1 µg/mL, levofloxacin 1 µg/mL, erythromycin 3 µg/mL in hydroalcoholic 50% solution); C6/36 cell line was cultured and infected according to Melo et al. [52]; *N. meningitidis* was grown at 37 °C under 5% of CO2 in agar GCB (Difco). C6/36 or M059J were used to replicate ZIKV when cell confluence achieved 70%. Aliquots of 1 mL ZIKV were prepared when viral cytopathic effect (CPE) reached until 75%, and were stored at − 86 °C.

OMVs extraction and OMV-ZIKV conjugated prototype

Preparation of OMVs from *N. meningitidis* was performed according to Alves et al. [53] and stored at − 80 °C before use. Aiming to obtain the ZVp, ZIKV grown in C6/36 were used to infect M059J cells; soon after ZIKV was fused with OMV vesicles from *N. meningitidis*. For this, different concentrations of OMV were added to M059J ZIKV-infected cells during different times points, in order to obtain the best attenuated ZIKV preparation. The resulting supernatants containing OMV fused with ZIKV were collected and inactivated at 56 °C for 1 h. Nano tracking analysis (Zetasizer Nano) was used to analyze the prototype (ZVp) preparations.

Cell culture and attenuated ZIKV prototype treatment

Human malignant U-251 glioblastoma cells (SIGMA product no. 09063001), provided by Professor Marcelo Lancellotti, were seeded in T-25 culture flasks, cultured in RPMI 1640 medium and incubated at 37 °C with 5% of CO_2. Upon 80% of confluence, each test flask (attenuated ZIKV group) was submitted to treatment with 1×10^{10} ZVp mL^{-1}, while the control group (CT) underwent the same conditions, except for prototype treatment. The experiment resulted in three biological replicates for each condition studied. Optical microscopic examinations were performed at 24 and 48 h post-treatment and a Zeiss Observer A1 microscope was used to capture bright field images, which were processed by Zeiss' AxioVision 4 software. After each time point of treatment, the cells were detached from each flask surface through trypsinization and submitted to sample preparation according to Melo et al. [35]. At last, the analytical technique of choice was mass spectrometry, which was performed with electrospray ionization and direct injection into a high-resolution mass spectrometer (ESI-HRMS).

Mass spectrometry analysis

After sample preparation, the analytical technique of choice was mass spectrometry, which was performed through electrospray ionization and direct injection into a high-resolution mass spectrometer (ESI-HRMS). Spectra were acquired using an ESI-LTQ-XL Orbitrap Discovery (Thermo Scientific, Bremen, Germany) with a nominal resolution of 30,000 (FWHM). The sample's ions were analyzed at the mass range of 400–1100 m/z, in the negative ion mode, comprising a total of five analytical replicates per group. Spectra were analyzed using XCalibur software (v. 2.4, Thermo Scientific, San Jose, CA).

Cellular death assays and cytokine real-time PCR

The experiments involving the glioma death were performed as follows: DNA fragmentation and morphological cells analysis were made by agarose gels staining with ethidium bromide and Wright staining viewed in light microscopy, respectively. The TNFα production was performed by qRTPCR using as endogenous control the GAPDH gene.

Statistical analysis

The method of choice to investigate differences between groups was Partial least squares discriminant analysis (PLS-DA), a statistical method that uses multivariate regression techniques to extract variables that may evidence these differences. The selection of ions which were characteristic for each group was carried out based on the impact that each feature presents in the model, i.e. the analysis of variable importance in projection (VIP) scores. The important chemical markers for each group were selected based in cutoff threshold established as a VIP score greater than 3.1. PLS-DA and VIP scores analysis were performed using the online software MetaboAnalyst 3.0 [54, 55].

TNF-alpha mRNA semi-quantification was performed through ANOVA and experiments were performed in triplicate for all evaluated groups, which were: CT, OMV and ZVP. The data shown in the graphs represent the means ± standard errors.

In vitro antiproliferative assay

The anti-proliferative activity of ZVp was investigated over glioblastoma cells (U251). Aiming to verify the potential of using attenuated ZIKV for control of tumors in general, seven other human cancer cell lines were also evaluated (MCF-7 = breast; NCI-ADR/RES = multidrug resistant ovarian; 786-O = kidney; NCI-H460 = lung, non-small cells; PC-3 = prostate; OVCAR-03 = ovarian; HT-29 = colon). Tumor cell lines were kindly provided by Frederick Cancer Research & Development Center, National Cancer Institute, Frederick, MA, USA. Cell proliferation was also evaluated using a non-tumor cell line HaCat (immortalized human keratinocytes), kindly provided by Dr. Ricardo Della Coletta (University of Campinas- UNICAMP, Brazil).

Stock cultures were grown according to Roman Junior et al. [56] and the attenuated ZIKV (1.18×10^9 OMV mL^{-1}) was prepared directly diluted in the complete medium, affording the final concentrations of 0.59, 5.9, 59 and 590×10^6 OMV mL^{-1}. Doxorubicin (final concentrations of 0.025, 0.25, 2.5 and 25 μg mL^{-1} in complete medium) was used as positive control.

Cells in 96-well plates (100 μL $well^{-1}$, inoculation density: $3.5–6 \times 10^4$ cell mL^{-1}) were exposed to different concentrations of sample and control (100 μL $well^{-1}$) in triplicate, for 48 h at 37 °C and 5% of CO_2. The anti-proliferative test and the colorimetric assay were performed according to Monks and Skehan, respectively, and GI_{50} values were determined using Shoemaker software [57–59]. The selectivity index (SI) was calculated according to Muller and Milton [60].

Additional file

Additional file 1: Figure S1. Optical microscopic analysis of U-251 cells under Wright staining. **Figure S2.** DNA fragmentation assay. **Figure S3.** Expression of TNF-alpha in U-251 glioblastoma cells. **Figure S4.** Statistical evidences of metabolomics differences between Control and ZVp treated groups. **Figure S5.** Anti-proliferative profile of ZVp against a panel of human tumor and non-tumor cell lines. **Table S1.** Antiproliferative effect of attenuated ZIKV prototype (ZVp) against a panel of human tumoral and non-tumoral cell lines expressed as GI50 and selectivity index. **Table S2.** Lipid chemical markers elected by PLS-DA VIP scores for U-251 glioblastoma cells after 24 hours of attenuated ZIKV-prototype (ZVp) treatment (negative ion mode).

Abbreviations

CT: control group; ESI-HRMS: electrospray ionization and high-resolution mass spectrometer; GBM: glioblastoma; hNPCs: human neural progenitor cells; hNSCs: human neural stem cells; MS: methionine synthase; *m/z*: mass/ion charge; NS: non-structural protein; OMV: outer membrane vesicles; PLS-DA: partial least squares discriminant analysis; SI: selectivity index; VIP score: variable importance in projection score; ZIKV: Zika virus; ZVp: Zika virus prototype.

Authors' contributions

ML was responsible for ZVp development, maintenance of cellular culture and ZVp administration on glioblastoma cells. MZD and EOL performed sample collection, mass spectrometry experiments and wrote the manuscript. MZD, EOL and DAD were responsible for microscopic analysis and photographs. ALTGR and GG conducted the anti-proliferative tests. MZD, EOL and DNO wrote the manuscript. DNO, CFORM, TMG and KNM performed data analysis and manuscript review. RRC idealized all experiments and managed the research group. MZD, EOL and DNO contributed equally during the research development and conclusion. All authors read and approved the final manuscript.

Author details

[1] Innovare Biomarkers Laboratory, School of Pharmaceutical Sciences, University of Campinas-UNICAMP, Campinas, SP, Brazil. [2] Laboratory of Biotechnology, School of Pharmaceutical Sciences, University of Campinas-UNICAMP, Campinas, SP, Brazil. [3] Faculty of Pharmaceutical Sciences, University of Campinas-UNICAMP, Campinas, SP 13081-970, Brazil. [4] Renal Pathophysiology Laboratory, Faculty of Medical Sciences, University of Campinas-UNICAMP, Campinas, SP, Brazil.

Acknowledgements

Innovare Laboratory would like to thank Professor Edson Durigon for providing the ZIKV strain used in this study and Professor José Butori Lopes de Faria for providing the infrastructure of the microscopy lab of the Microdiabetes Laboratory at the Faculty of Medical Sciences (Unicamp), which was essential for cell imaging.

Competing interests

The authors declare that they have no competing interests.

Availability of data and materials

The datasets used and/or analyzed during the current study are available from the corresponding author on reasonable request.

Consent for publication

Not applicable.

Ethics approval and consent to participate

Not applicable.

Funding

This work was supported by the OCRC (Obesity Comorbidities Research Center) CEPID: CMPO - Centro Multidisciplinar de Pesquisa em Obesidade e Doenças Associadas (FAPESP number: 13/07607-8); the National Council for

Scientific and Technological Development (134522/2016-8) for the fellowship from MZD; the Coordination for the Improvement of Higher Level Personnel (CAPES) for the fellowships from EOL (PNPD: 1578388) and TMG (PROEX: 1489740); by São Paulo Research Foundation (FAPESP, Process Nos. 11/50400-0, 15/06809-1 and 18/14657-5 for RRC, and 16/17066-2 for CFORM); and by Plano Nacional de Enfrentamento ao Aedes aegypti e à Microcefalia [Brazilian Plan for Fighting Aedes aegypti and Microcephaly] for the fellowship under process No. 88887.137889/2017-00 for DNO.

Publisher's Note

Received: 28 February 2018 Accepted: 3 August 2018
Published online: 04 September 2018

References

1. de Oliveira WK. Increase in reported prevalence of microcephaly in infants born to women living in areas with confirmed Zika virus transmission during the first trimester of pregnancy—Brazil, 2015. MMWR Morb Mortal Wkly Rep. 2016;65:242–7.
2. Brasil P, Pereira JP Jr, Moreira ME, Ribeiro Nogueira RM, Damasceno L, Wakimoto M, Rabello RS, Valderramos SG, Halai U-A, Salles TS. Zika virus infection in pregnant women in Rio de Janeiro. N Engl J Med. 2016;2016(375):2321–34.
3. Tang H, Hammack C, Ogden SC, Wen Z, Qian X, Li Y, Yao B, Shin J, Zhang F, Lee EM. Zika virus infects human cortical neural progenitors and attenuates their growth. Cell Stem Cell. 2016;18(5):587–90.
4. McGrath EL, Rossi SL, Gao J, Widen SG, Grant AC, Dunn TJ, Azar SR, Roundy CM, Xiong Y, Prusak DJ. Differential responses of human fetal brain neural stem cells to Zika virus infection. Stem cell Rep. 2017;8(3):715–27.
5. Devhare P, Meyer K, Steele R, Ray RB, Ray R. Zika virus infection dysregulates human neural stem cell growth and inhibits differentiation into neuroprogenitor cells. Cell Death Dis. 2017;8(10):e3106.
6. Zhu Z, Gorman MJ, McKenzie LD, Chai JN, Hubert CG, Prager BC, Fernandez E, Richner JM, Zhang R, Shan C. Zika virus has oncolytic activity against glioblastoma stem cells. J Exp Med. 2017;214(10):2843–57.
7. Lima EO, Guerreiro TM, Melo CFOR, de Oliveira DN, Machado D, Lancelloti M, Catharino RR. MALDI imaging detects endogenous digoxin in glioblastoma cells infected by Zika virus—Would it be the oncolytic key? J Mass Spectrom. 2018;53(3):257–63. https://doi.org/10.1002/jms.4058.
8. Russell SJ, Peng KW, Bell JC. Oncolytic virotherapy. Nat Biotechnol. 2012;30(7):658–70.
9. Zeyaullah M, Patro M, Ahmad I, Ibraheem K, Sultan P, Nehal M, Ali A. Oncolytic viruses in the treatment of cancer: a review of current strategies. Pathol Oncol Res. 2012;18(4):771–81.
10. Wright SC, Kumar P, Tam AW, Shen N, Varma M, Larrick JW. Apoptosis and DNA fragmentation precede TNF-induced cytolysis in U937 cells. J Cell Biochem. 1992;48(4):344–55.
11. Elias L, Berry C. Induction of differentiation by tumour necrosis factor in HL-60 cells is associated with the formation of large DNA fragments. Leukemia. 1991;5(10):879–85.
12. Balkwill F. Tumour necrosis factor and cancer. Nat Rev Cancer. 2009;9(5):361.
13. Carswell E, Old LJ, Kassel R, Green S, Fiore N, Williamson B. An endotoxin-induced serum factor that causes necrosis of tumors. Proc Natl Acad Sci. 1975;72(9):3666–70.
14. Chang HY, Yang X. Proteases for cell suicide: functions and regulation of caspases. Microbiol Mol Biol Rev. 2000;64(4):821–46.
15. Dang J, Tiwari SK, Lichinchi G, Qin Y, Patil VS, Eroshkin AM, Rana TM. Zika virus depletes neural progenitors in human cerebral organoids through activation of the innate immune receptor TLR3. Cell Stem Cell. 2016;19(2):258–65.
16. Yaddanapudi K, De Miranda J, Hornig M, Lipkin WI. Toll-like receptor 3 regulates neural stem cell proliferation by modulating the Sonic Hedgehog pathway. PLoS ONE. 2011;6(10):e26766.
17. Kataoka T, Budd RC, Holler N, Thome M, Martinon F, Irmler M, Burns K, Hahne M, Kennedy N, Kovacsovics M, et al. The caspase-8 inhibitor FLIP promotes activation of NF-kappaB and Erk signaling pathways. Curr Biol. 2000;10(11):640–8.
18. Roberts PJ, Der CJ. Targeting the Raf-MEK-ERK mitogen-activated protein kinase cascade for the treatment of cancer. Oncogene. 2007;26(22):3291–310.
19. Gu XX, Tsai CM. Purification of rough-type lipopolysaccharides of *Neisseria meningitidis* from cells and outer membrane vesicles in spent media. Anal Biochem. 1991;196(2):311–8.
20. Park HS, Jung HY, Park EY, Kim J, Lee WJ, Bae YS. Cutting edge: direct interaction of TLR4 with NAD (P) H oxidase 4 isozyme is essential for lipopolysaccharide-induced production of reactive oxygen species and activation of NF-κB. J Immunol. 2004;173(6):3589–93.
21. Asehnoune K, Strassheim D, Mitra S, Kim JY, Abraham E. Involvement of reactive oxygen species in Toll-like receptor 4-dependent activation of NF-κB. J Immunol. 2004;172(4):2522–9.
22. Boje KM, Arora PK. Microglial-produced nitric oxide and reactive nitrogen oxides mediate neuronal cell death. Brain Res. 1992;587(2):250–6.
23. Chao CC, Hu S, Peterson PK. Glia, cytokines, and neurotoxicity. Crit Rev Neurobiol. 1995;9(2–3):189–205.
24. Fadok VA, Voelker DR, Campbell PA, Cohen JJ, Bratton DL, Henson PM. Exposure of phosphatidylserine on the surface of apoptotic lymphocytes triggers specific recognition and removal by macrophages. J Immunol. 1992;148(7):2207–16.
25. Fadok VA, Bratton DL, Rose DM, Pearson A, Ezekewitz RAB, Henson PM. A receptor for phosphatidylserine-specific clearance of apoptotic cells. Nature. 2000;405:85.
26. Li J, Baud O, Vartanian T, Volpe JJ, Rosenberg PA. Peroxynitrite generated by inducible nitric oxide synthase and NADPH oxidase mediates microglial toxicity to oligodendrocytes. Proc Natl Acad Sci USA. 2005;102(28):9936–41.
27. Koprowski H, Zheng YM, Heber-Katz E, Fraser N, Rorke L, Fu ZF, Hanlon C, Dietzschold B. In vivo expression of inducible nitric oxide synthase in experimentally induced neurologic diseases. Proc Natl Acad Sci. 1993;90(7):3024–7.
28. Danishpajooh IO, Gudi T, Chen Y, Kharitonov VG, Sharma VS, Boss GR. Nitric oxide inhibits methionine synthase activity in vivo and disrupts carbon flow through the folate pathway. J Biol Chem. 2001;276(29):27296–303.
29. Banerjee RV, Matthews RG. Cobalamin-dependent methionine synthase. FASEB J. 1990;4(5):1450–9.
30. James SJ, Cross DR, Miller BJ. Alterations in nucleotide pools in rats fed diets deficient in choline, methionine and/or folic acid. Carcinogenesis. 1992;13(12):2471–4.
31. Dean W, Lucifero D, Santos F. DNA methylation in mammalian development and disease. Birth Defects Res C Embryo Today. 2005;75(2):98–111.
32. Guo H, Lishko VK, Herrera H, Groce A, Kubota T, Hoffman RM. Therapeutic tumor-specific cell cycle block induced by methionine starvation in vivo. Can Res. 1993;53(23):5676–9.
33. James SJ, Miller BJ, McGarrity LJ, Morris SM. The effect of folic acid and/or methionine deficiency on deoxyribonucleotide pools and cell cycle distribution in mitogen-stimulated rat lymphocytes. Cell Prolif. 1994;27(7):395–406.
34. Tuck-Muller C, Narayan A, Tsien F, Smeets D, Sawyer J, Fiala E, Sohn O, Ehrlich M. DNA hypomethylation and unusual chromosome instability in cell lines fromICF syndrome patients. Cytogenet Genome Res. 2000;89(1–2):121–8.
35. Melo CFO, Delafiori J, de Oliveira DN, Guerreiro TM, Esteves CZ, Lima EDO, Pando-Robles V, Catharino RR, Milanez GP, do Nascimento GM. Serum metabolic alterations upon Zika infection. Front Microbiol. 1954;2017:8.
36. Polumuri SK, Toshchakov VY, Vogel SN. Role of phosphatidylinositol-3 kinase in transcriptional regulation of TLR-induced IL-12 and IL-10 by Fcγ receptor ligation in murine macrophages. J Immunol. 2007;179(1):236–46.
37. Weichhart T, Säemann MD. The PI3K/Akt/mTOR pathway in innate immune cells: emerging therapeutic applications. Ann Rheum Dis. 2008;67(Suppl 3):70–4.
38. Dello Russo C, Lisi L, Tringali G, Navarra P. Involvement of mTOR kinase in cytokine-dependent microglial activation and cell proliferation. Biochem Pharmacol. 2009;78(9):1242–51.

39. Liang Q, Luo Z, Zeng J, Chen W, Foo SS, Lee SA, Ge J, Wang S, Goldman SA, Zlokovic BV, et al. Zika virus NS4A and NS4B proteins deregulate Akt-mTOR signaling in human fetal neural stem cells to inhibit neurogenesis and induce autophagy. Cell Stem Cell. 2016;19(5):663–71.
40. Streit WJ. Microglia as neuroprotective, immunocompetent cells of the CNS. Glia. 2002;40(2):133–9.
41. Raivich G, Bohatschek M, Kloss CU, Werner A, Jones LL, Kreutzberg GW. Neuroglial activation repertoire in the injured brain: graded response, molecular mechanisms and cues to physiological function. Brain Res Rev. 1999;30(1):77–105.
42. Das AK, Hajra AK. Quantification, characterization and fatty acid composition of lysophosphatidic acid in different rat tissues. Lipids. 1989;24(4):329–33.
43. Tigyi G, Hong L, Yakubu M, Parfenova H, Shibata M, Leffler CW. Lysophosphatidic acid alters cerebrovascular reactivity in piglets. Am J Physiol Heart Circ Physiol. 1995;268(5):H2048–55.
44. Natarajan V, Taher MM, Roehm B, Parinandi NL, Schmid H, Kiss Z, Garcia J. Activation of endothelial cell phospholipase D by hydrogen peroxide and fatty acid hydroperoxide. J Biol Chem. 1993;268(2):930–7.
45. Boyer CS, Bannenberg GL, Neve EP, Ryrfeldt Å, Moldéus P. Evidence for the activation of the signal-responsive phospholipase A2 by exogenous hydrogen peroxide. Biochem Pharmacol. 1995;50(6):753–61.
46. Brault S, Gobeil F, Fortier A, Honoré JC, Joyal JS, Sapieha PS, Kooli A, Martin É, Hardy P, Ribeiro-da-Silva A. Lysophosphatidic acid induces endothelial cell death by modulating the redox environment. Am J Physiol Regul Integr Comp Physiol. 2007;292(3):R1174–83.
47. Dong Y, Wu Y, Cui MZ, Xu X. Lysophosphatidic acid triggers apoptosis in HeLa cells through the upregulation of tumor necrosis factor receptor superfamily member 21. Mediators Inflamm. 2017. https://doi.org/10.1155/2017/2754756.
48. Olmo IG, Carvalho TG, Costa VV, Alves-Silva J, Ferrari CZ, Izidoro-Toledo TC, da Silva JF, Teixeira AL, Souza DG, Marques JT. Zika virus promotes neuronal cell death in a non-cell autonomous manner by triggering the release of neurotoxic factors. Front immunol. 1016;2017:8.
49. Matheron S, d'Ortenzio E, Leparc-Goffart I, Hubert B, de Lamballerie X, Yazdanpanah Y. Long-lasting persistence of Zika virus in semen. Clin infect Dis. 2016;63(9):1264.
50. Nicastri E, Castilletti C, Liuzzi G, Iannetta M, Capobianchi MR, Ippolito G. Persistent detection of Zika virus RNA in semen for six months after symptom onset in a traveller returning from Haiti to Italy, February 2016. Euro Surveill. 2016. https://doi.org/10.2807/1560-7917.ES.2016.21.32.30314.
51. Davidson A. Suspected female-to-male sexual transmission of Zika virus—New York City, 2016. MMWR Morb Mortal Wkly Rep. 2016;65:716–7.
52. Melo CFOR, de Oliveira DN, de Oliveira Lima E, Guerreiro TM, Esteves CZ, Beck RM, Padilla MA, Milanez GP, Arns CW, Proença-Modena JL. A Lipidomics approach in the characterization of Zika-infected mosquito cells: potential targets for breaking the transmission cycle. PLoS ONE. 2016;11(10):e0164377.
53. Alves D, Mattos I, Hollanda L, Lancellotti M. Use of mesoporous silica Sba-15 and Sba-16 in association of outer membrane vesicles-Omv from *Neisseria meningitidis*. J Vaccines Vaccin. 2013. https://doi.org/10.4172/2157-7560.1000196.
54. Xia J, Wishart DS. Web-based inference of biological patterns, functions and pathways from metabolomic data using MetaboAnalyst. Nat Protoc. 2011;6(6):743–60.
55. Xia J, Wishart DS. Using metaboanalyst 3.0 for comprehensive metabolomics data analysis. Curr Protoc Bioinform. 2016;55:14.10.11–91.
56. Roman Junior WA, Gomes DB, Zanchet B, Schönell AP, Diel KA, Banzato TP, Ruiz AL, Carvalho JE, Neppel A, Barison A. Antiproliferative effects of pinostrobin and 5,6-dehydrokavain isolated from leaves of *Alpinia zerumbet*. Revista Brasileira de Farmacognosia. 2017;27(5):592–8.
57. Monks A, Scudiero D, Skehan P, Shoemaker R, Paull K, Vistica D, Hose C, Langley J, Cronise P, Vaigro-Wolff A. Feasibility of a high-flux anticancer drug screen using a diverse panel of cultured human tumor cell lines. JNCI. 1991;83(11):757–66.
58. Skehan P, Storeng R, Scudiero D, Monks A, McMahon J, Vistica D, Warren JT, Bokesch H, Kenney S, Boyd MR. New colorimetric cytotoxicity assay for anticancer-drug screening. JNCI. 1990;82(13):1107–12.
59. Shoemaker RH. The NCI60 human tumour cell line anticancer drug screen. Nat Rev Cancer. 2006;6(10):813–23.
60. Muller PY, Milton MN. The determination and interpretation of the therapeutic index in drug development. Nat Rev Drug Discov. 2012;11(10):751–61.